J Mater Sci (2011) 46:4354–4360
DOI 10.1007/s10853-010-5103-2

IIB 2010

Cation off-stoichiometric $SrMnO_{3-\delta}$ thin film grown by pulsed laser deposition

S. Kobayashi · Y. Tokuda · T. Ohnishi · T. Mizoguchi · N. Shibata · Y. Sato · Y. Ikuhara · T. Yamamoto

Received: 10 September 2010 / Accepted: 20 November 2010 / Published online: 14 December 2010

Abstract The laser energy density (laser fluence) dependency of the Sr/Mn ratio was investigated for $SrMnO_{3-\delta}$ (SMO) thin films grown by pulsed laser deposition (PLD). It was found that the Sr/Mn ratio showed a steep increase followed by a gradual increase as the laser fluence was increased. However, the Sr/Mn ratio always showed Mn-excess under the present laser fluence condition as long as stoichiometric $SrMnO_3$ targets were used. In order to obtain cation stoichiometric SMO films, it was necessary to use Sr-excess $SrMnO_3$ targets in addition with laser fluence tuning. The crystal quality of the SMO thin film was found to vary with the Sr/Mn ratio. In stoichiometric or Sr-excess SMO thin films, epitaxial thin films could be obtained, whereas Mn-excess thin films showed very low crystallinity. Sr-excess films were also found to have some extra SrO planes. In addition, they exhibited out-of-plane lattice expansion which electron energy loss spectroscopy analysis revealed was due to Mn vacancies. The variation of film growth was closely related to point defects due to excess cations included in growing thin films.

S. Kobayashi · Y. Tokuda · T. Yamamoto
Department of Advanced Materials Science, University of Tokyo, Kashiwa 277-8561, Japan

S. Kobayashi (✉)
Department of Advanced Materials Science, University of Tokyo, 2-11-16 Yayoi, Bunkyo, Tokyo 113-8656, Japan
e-mail: kobayashi@sigma.t.u-tokyo.ac.jp

T. Ohnishi
National Institute for Materials Science, Tsukuba 305-0047, Japan

T. Mizoguchi
Institute of Industrial Science, University of Tokyo, Tokyo 153-8505, Japan

N. Shibata · Y. Sato · Y. Ikuhara
Institute of Engineering Innovation, University of Tokyo, Tokyo 113-8656, Japan

Introduction

Pulsed laser deposition (PLD) is widely used for oxide thin film growth because it has been considered easy to obtain oxide thin films with the same composition as that of the target materials. However, Ohnishi et al. [1, 2] pointed out that the composition of $SrTiO_3$ (STO) films, specifically the Sr/Ti ratio, depends on the laser energy density on targets (laser fluence). Namely, cation stoichiometric STO films can be obtained only at critical laser fluence, while cation off-stoichiometric STO films exhibit lattice expansion, which results from the incorporation of point defects due to excess Sr or Ti [3]. Variation of the Sr/Ti ratio can change physical properties of the films. For example, off-stoichiometric homo-epitaxial STO films are considered to become ferroelectric at room temperature, whereas stoichiometric STO does not exhibit ferroelectricity at any temperature [4, 5]. Thus, it is very important to control the cation ratio in complex oxide films by PLD. However, there are very few reports about the cation off-stoichiometry in PLD-grown complex oxide thin films.

In this study, we focus on $SrMnO_{3-\delta}$ (SMO) thin films. SMO is a perovskite-type manganese oxide, which is often used as an end member of $La_{1-x}Sr_xMnO_3$ (LSMO)-series colossal magnetoresistance (CMR) materials [6]. $LaMnO_3$/$SrMnO_3$ superlattices have been intensively investigated to observe different phenomena from $La_{1-x}Sr_xMnO_3$ single crystals [7, 8]. However, there have been very few reports on SMO thin films, despite the fact that it has attractive

possibilities for showing interesting properties due to mixed oxidation states or strain induced by the mismatch with the substrate [9–13]. Thus, we grew SMO thin films by PLD to investigate the Sr/Mn ratio change with laser fluence, their microstructure, and the Mn oxidation states by high-resolution transmission electron microscopy (HRTEM), scanning transmission electron microscopy (STEM) using an aberration corrector, and electron energy loss spectroscopy (EELS).

Experimental procedure

SMO films with various cation off-stoichiometry were grown on atomically flat single crystal STO (001) substrates by PLD. The substrate temperature was kept at 800 °C, and the base pressure before the film growth was set around $\sim 5 \times 10^{-8}$ Torr. The incident angle of the laser on the target was 45°, and the distance between the target and the substrate was set at 50 mm. The film thickness was controlled by total pulse counts to be about 200 nm using a KrF excimer laser (248 nm) at a laser frequency of 2 Hz. The off-stoichiometry, i.e., the Sr/Mn ratio, was tuned by changing the laser fluence and the target composition. Laser fluence was changed by a reflection-type variable attenuator system without any change of the spot size and a laser discharge voltage. The Sr/Mn ratios of the polycrystalline SMO targets used were 50/50, 56/44, 59/41, and 62/38. Sufficient preablation of the surface of these targets was performed before the film growth. To obtain SMO thin films with an expected Sr/Mn ratio, the laser fluence dependency of the Sr/Mn ratio was determined by energy dispersive X-ray spectroscopy (EDS) on a scanning electron microscope using amorphous films prepared on aluminum substrates at room temperature. With the obtained dependency, crystalline SMO films with the aimed Sr/Mn ratios were grown under the growth condition described above. After the film growth, the actual Sr/Mn ratio was confirmed again by EDS in HRTEM (EM-002BF, TOPCON Co.). In the determination of the Sr/Mn ratio in the grown films, a stoichiometric SMO polycrystal, which was glued on the films, was used as a standard material for the compositional analysis.

Lattice parameters were measured by X-ray diffractometry (XRD, ATX-G, Rigaku Co). X-ray reciprocal space mapping was performed around 114 Bragg reflections from the STO substrate.

The obtained films were observed by HRTEM and STEM (JEM-2100F, JEOL Ltd) equipped with an aberration corrector (CEOS GmbH), both operated at 200 kV. The observation was carried out in a cross-sectional view of the films. The Radial Wiener Filter was applied to HRTEM and STEM images to reduce the noise by commercial software in Digital Micrograph (Gatan Inc) [14]. Thin foils for HRTEM and STEM observation were prepared by conventional procedures including cutting, mechanical grinding, polishing, dimple grinding, and Ar-ion beam milling for electron transparency. Ar-ion beam milling was performed with PIPS^{TM} (Model 691, Gatan Inc).

STEM EELS (Model 766 Enfina, Gatan Inc) was used to analyze the local electronic states in the films. Quantitative analysis of the Mn-$L_{2,3}$ edges was conducted by a Hartree–Slater function in Digital Micrograph. In addition, to obtain information about standard O–K and Mn-$L_{2,3}$ edges, orthorhombic $SrMnO_{2.5}$ and cubic $SrMnO_3$ polycrystals with Mn oxidation states of 3+ and 4+ , respectively, were prepared by sintering. $SrMnO_{2.5}$ polycrystals were fired at 1240 °C for 12 h in $\sim 3 \times 10^{-3}$ Torr vacuum atmosphere and quenched in oil. Cubic $SrMnO_3$ polycrystals were obtained by annealing $SrMnO_{2.5}$ polycrystals to remove the oxygen vacancies at 350 °C for 12 h in air [15–17]. The lattice parameters of the two polycrystals were confirmed by XRD [15, 18].

Results

Figure 1 shows the laser fluence dependency of the Sr/Mn ratio in SMO thin films which were grown using the targets with various Sr/Mn ratios. In the plots, there are two major distinct features. One is that the Sr/Mn ratio in the obtained films exhibits laser fluence dependency. As seen for the stoichiometric SMO (Sr/Mn = 50/50) target, the Sr/Mn ratio steeply increases with laser fluence up to around 0.3 J cm^{-2} and then gradually increases for laser fluence higher than 0.3 J cm^{-2}. The other feature is that the Sr/Mn

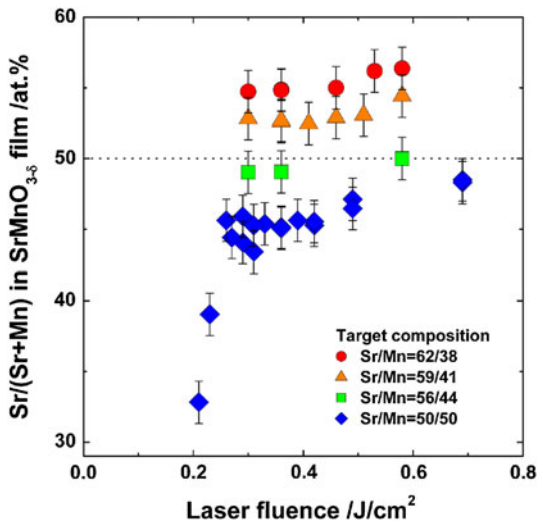

Fig. 1 (Color online) Dependency of the Sr/Mn ratio on laser fluence in $SrMnO_{3-\delta}$ films. Four kinds of polycrystalline $SrMnO_3$ targets were used, with Sr/Mn ratios 50/50, 56/44, 59/41, and 62/38

ratio of the films is always lower than 1.0 (Mn-excess) under the present laser fluence condition as long as a stoichiometric target is used. To obtain stoichiometric SMO thin films, we have to select the target with suitable off-stoichiometric Sr/Mn ratio in addition to tuning the laser fluence to an optimal value. These features obtained in SMO are very different from the case reported in STO homo-epitaxial film growth [2]. In case of STO films grown by PLD, the cation (Sr/Ti) ratio strongly depends on laser fluence. In contrast, the dependency is very weak in the present case of SMO. In addition, the Sr/Mn ratio of the SMO films obtained from the stoichiometric target is always smaller than 1.0 (Mn-excess), i.e., stoichiometric SMO films could not be obtained from stoichiometric SMO targets under the conditions used in this study.

Out-of-plane X-ray diffraction (XRD) patterns of SMO thin films around the 002 peak are shown in Fig. 2a. In the figure, XRD profiles obtained from the SMO films with different Sr/Mn ratios, specifically 56/44, 53/47, 50/50, and 45/55, are presented. The laser fluences used for the growth of these films were 0.58 J cm^{-2} (Sr/Mn = 56/44), 0.46 J cm^{-2} (Sr/Mn = 53/47), 0.58 J cm^{-2} (Sr/Mn = 50/50), and 0.36 J cm^{-2} (Sr/Mn = 45/55), and the spot size used in this study was 0.05 cm^2. As seen in the XRD profiles, the out-of-plane lattice parameter increases as the Sr/Mn ratio increases. The crystal quality of SMO thin film is closely related to the Sr/Mn ratio. The crystallinity degraded with excess Mn ratio (Sr/Mn = 45/55) while epitaxial thin films could be obtained with the composition of Sr/Mn = 1 or a slight Sr-excess ratio. Hereafter, we focus on stoichiometric and Sr-excess SMO thin films with the composition ratios of Sr/Mn = 50/50, 53/47, and 56/44.

Figure 2b shows an example of a reciprocal space mapping taken around 114 reflections of the SMO film whose Sr/Mn ratio is 56/44. The in-plane lattice parameter of the SMO film is similar to that of the STO substrate in spite of showing lattice expansion normal to the substrate surface. Similar tendencies were also observed for other SMO thin films with Sr/Mn = 50/50 and 53/47.

Figure 3 shows bright-field TEM and HRTEM images of stoichiometric SMO film (Sr/Mn = 50/50), which are cross-sectional views along the [100] zone axis of the STO substrate. As seen in the electron diffraction patterns inset in Fig. 3a and the HRTEM image in (b), there are no secondary phases and amorphous phases in the film, indicating a good quality epitaxial thin film was obtained. However, dark contrast exists in the film region near the interface. The dark contrast is considered to relate to the existence of strain, which originates from the lattice mismatch between the STO substrate and the SMO film or cation defects due to a very small off-stoichiometry.

On the other hand, in the Sr-excess SMO thin film (Sr/Mn = 53/47), many line contrasts normal to the substrate

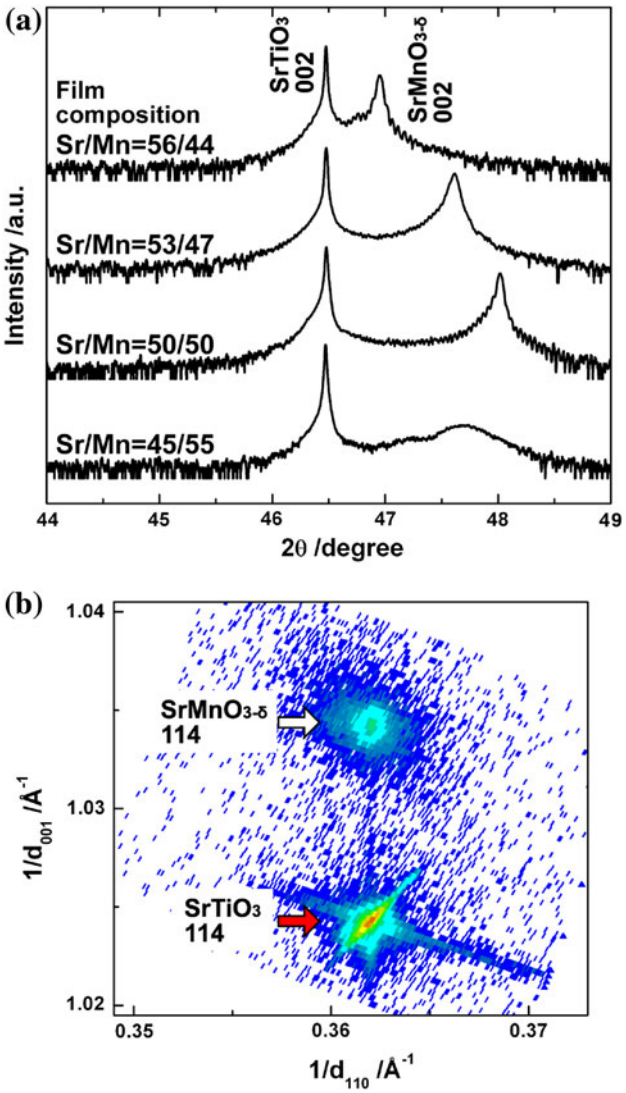

Fig. 2 (Color online) **a** Out-of-plane X-ray diffraction pattern in the vicinity of the $SrTiO_3$ 002 peak of $SrMnO_{3-\delta}$ thin films with the variation of the Sr/Mn ratio. **b** The reciprocal space mapping of $SrMnO_{3-\delta}$ thin film with Sr/Mn = 56/44. Here, Miller indices for SMO are based on the notation for fundamental perovskite units

surface were observed as shown in Fig. 4a and b. The appearance of the streak patterns normal to the line contrast is also confirmed in the electron diffraction pattern. These indicate that some planar defects are formed normal to the substrate surface. Considering the Sr/Mn ratio in Sr-excess films, the planar defects are due to extra SrO planes.

Figure 5a shows a high-angle annular dark-field (HAADF) STEM image taken from the area including the planar defect in the SMO film with Sr/Mn = 53/47. In the HAADF-STEM image, the intensity of atomic columns is approximately proportional to the square of the atomic number (Z) included in atomic columns, meaning that the intensity of Sr ($Z = 38$) atomic columns should be higher than that of Mn–O ($Z = 25$ and 8, respectively) atomic

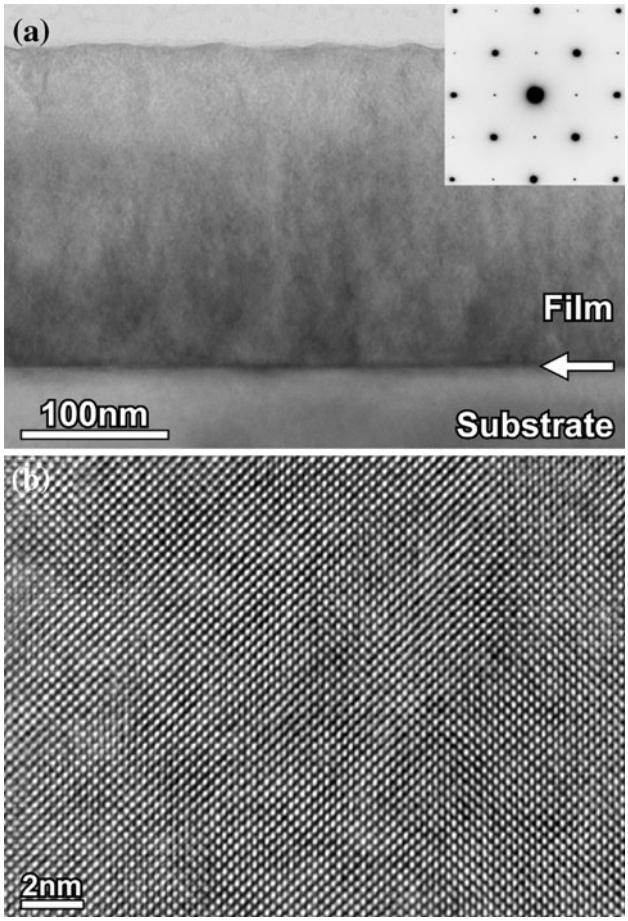

Fig. 3 **a** Cross-sectional bright-field TEM image of $SrMnO_{3-\delta}$ film with Sr/Mn = 50/50 and $SrTiO_3$ substrate. The *inset* shows a selected area electron diffraction pattern obtained from the film area, with contrast inversed for ease of viewing. The interface is denoted by the *white arrow*. **b** HRTEM image taken from a part of the same specimen in **a**. Both the images were taken along the [100] zone axis

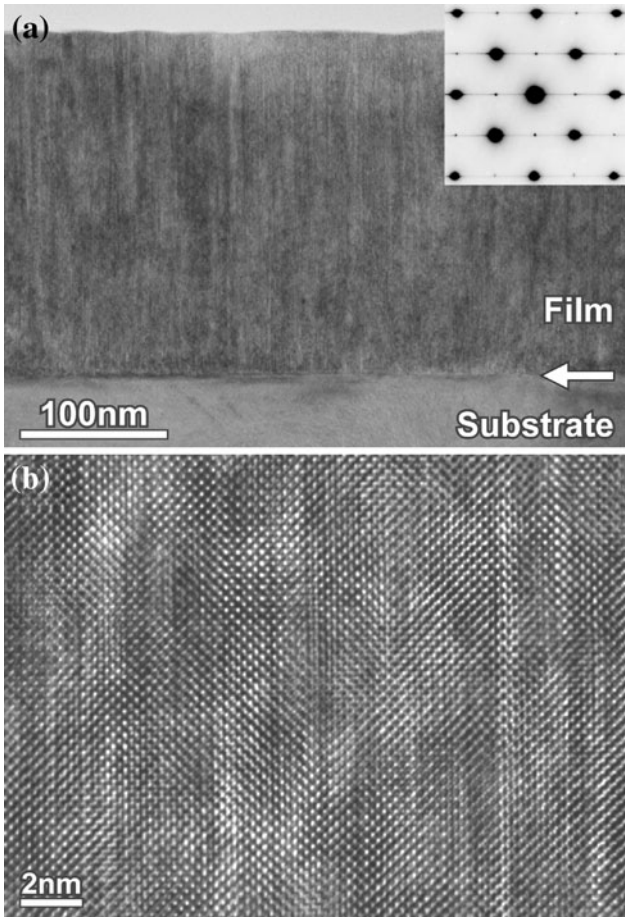

Fig. 4 **a** Cross-sectional bright-field TEM image of $SrMnO_{3-\delta}$ film with Sr/Mn = 53/47 and $SrTiO_3$ substrate. The *inset* shows a selected area electron diffraction pattern obtained from the film area, with contrast inversed for ease of viewing. The interface is denoted by the *white arrow*. **b** HRTEM image taken from a part of the same specimen in **a**. Both the images were taken along the [100] zone axis

columns in the SMO lattice [19]. Figure 5b shows an intensity profile taken from the HAADF-STEM image in Fig. 5a. In region A, two types of the intensity peaks can be seen, which correspond to Sr and Mn–O atomic column positions. In region B, the intensity difference in the two peaks becomes very weak. This can be understood as follows. When an extra SrO (100) plane is included into the perovskite structure as indicated by the schematic illustration of Fig. 5a, the SMO crystal is shifted by $a/2[011]$ (here, a is a lattice parameter of SMO) from the original region. When this structure is viewed along the [100] direction, Sr columns in the shifted region overlap with Mn–O columns in the original region, and vice versa. This leads to the image intensity features seen in region B. It is therefore considered that the observed line contrasts in Fig. 4 are due to the extra SrO planes.

As seen in Fig. 4, the extra SrO planes are formed perpendicularly to the substrate surface. When extra SrO planes are formed in the crystal, the lattice shows expansion in the stacking direction of SrO planes [20]. Since the lattice parameter of bulk $SrMnO_{3-\delta}$ ($0 \leq \delta \leq 0.5$) with a pseudocubic structure is smaller than that of STO (3.905 Å) [17, 21], in-plane lattice expansion of grown SMO film serves to decrease the lattice mismatch with the STO substrate. On the other hand, Sr-excess SMO films show out-of-plane lattice expansion as shown in Fig. 2. The out-of-plane lattice expansion is closely related to the incorporation of excess Sr into SMO lattice as discussed later.

Figure 6 shows O–K and Mn-$L_{2,3}$ EELS spectra taken from SMO films with Sr/Mn = 50/50 and 53/47. In the figures, the O–K and Mn-$L_{2,3}$ edges of $SrMnO_{3-\delta}$ ($\delta = 0$ and 0.5) polycrystals are also shown as standard edges for SMO including Mn^{3+} and Mn^{4+}. All the spectra are aligned so that the first peak of the O–K edges around 530 eV are at the same position. Features of the O–K and

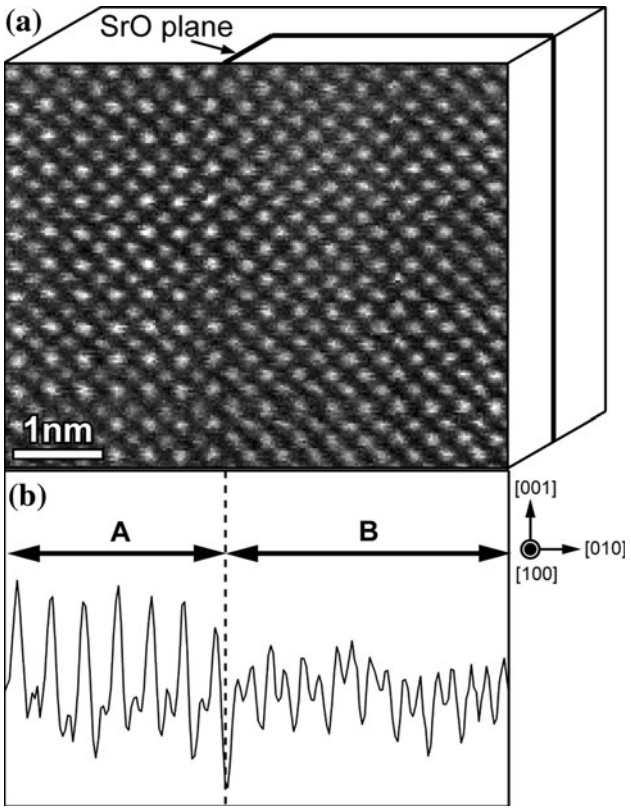

Fig. 5 a HAADF-STEM image of $SrMnO_{3-\delta}$ thin film with Sr/Mn = 53/47 taken along the [100] zone axis. The schematic of $SrMnO_{3-\delta}$ lattice including extra SrO plane is also shown. **b** An intensity profile taken from **a**. In the profile, the intensity is summed over the vertical direction

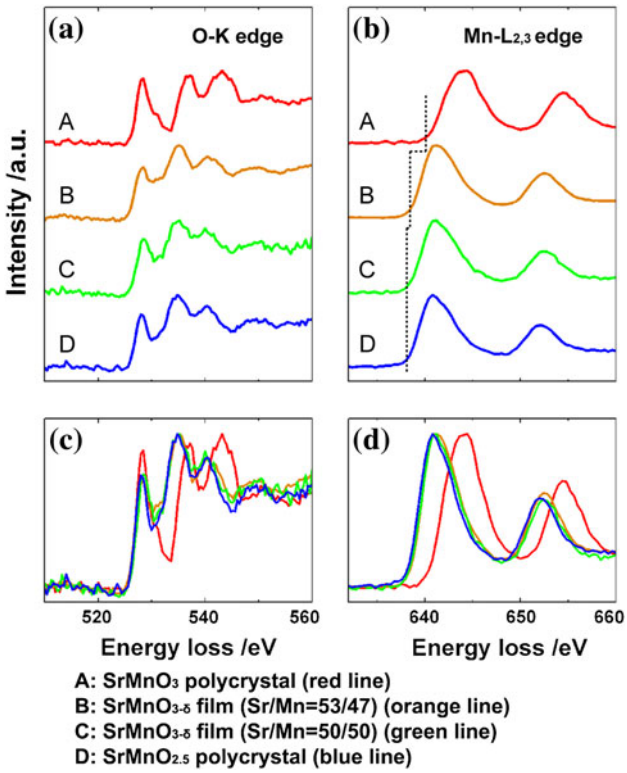

Fig. 6 (Color online) O–K edge **a** and Mn-$L_{2,3}$ edge **b** EELS spectra taken from $SrMnO_{3-\delta}$ films with Sr/Mn = 50/50 and 53/47, and $SrMnO_{3-\delta}$ ($\delta = 0$ and 0.5) polycrystals. The *dashed line* in **b** shows the onset of the Mn edges. These figures are rescaled in **c** and **d**, respectively

Mn-$L_{2,3}$ edges in $SrMnO_{3-\delta}$ films are very similar to those of $SrMnO_{2.5}$, suggesting that the oxidation state of Mn is likely to be 3+, which will be discussed later in detail, and SMO films grown in the present study include oxygen vacancies.

Discussion

The oxidation state of Mn can be understood by peak shifts of the Mn-$L_{2,3}$ edge as is clear for the $SrMnO_3$ and $SrMnO_{2.5}$ polycrystals (Fig. 6b). When the Mn-$L_{2,3}$ edge of the SMO (Sr/Mn = 50/50) film is compared with that of the SMO (Sr/Mn = 53/47) film, their peak positions are slightly different, indicating that the Mn oxidation state of the SMO (Sr/Mn = 53/47) film is different from that of the stoichiometric SMO (Sr/Mn = 50/50) film. To investigate more in detail, the Mn L_3/L_2 ratio was calculated. For the calculation, a Hartree–Slater function was used as a step function to extract the white line intensities [22]. The remaining signal under the corrected L_2 and L_3 lines was integrated by a window of 10 eV as shown in Fig. 7a. The integration area is ± 10 eV from the minimum position between the L_3 and L_2 edges, and a scaling window of 4 eV was used. The resulting integrated intensity was used to calculate the Mn L_3/L_2 ratio. The calculation results are shown in Fig. 7b with the results performed for SMO polycrystals. Here, we assumed that there is a linear relationship between the Mn L_3/L_2 ratio and the Mn oxidation state as indicated by dotted line in Fig. 7b. The result of SMO polycrystals is in good agreement with a previous report performed for other perovskite manganese oxides [22]. On the other hand, the Mn L_3/L_2 ratio of grown SMO films is found to increase with the increase of the Sr/Mn ratio. The Mn oxidation state is about 3.2+ in SMO film with Sr/Mn = 50/50, while it is about 3.4+ in SMO film with Sr/Mn = 53/47. The difference in the Mn oxidation state between SMO films with Sr/Mn = 50/50 and Sr/Mn = 53/47 is closely related to the cation off-stoichiometry. Figure 8 shows out-of-plane and in-plane lattice parameters obtained from SMO films with different Sr/Mn ratios. In-plane lattice parameters of all SMO thin films coincide with those of the STO substrate whereas out-of-plane parameters increase as the Sr/Mn ratios increase. It is assumed that

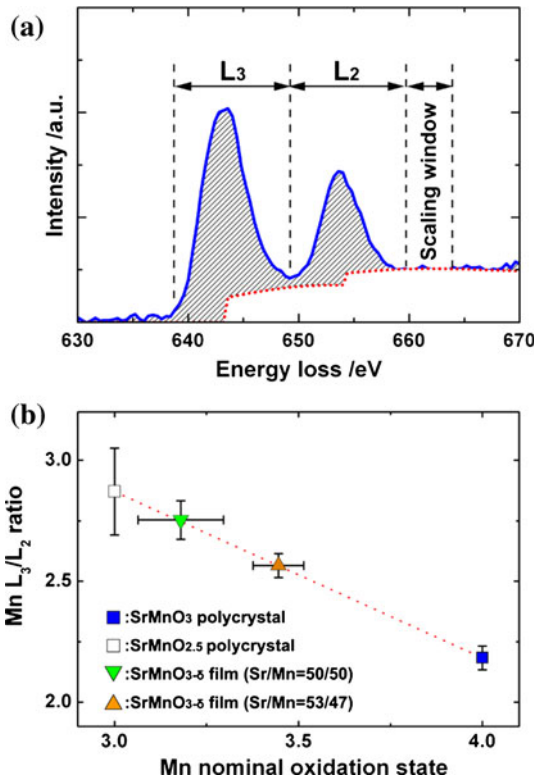

Fig. 7 (Color online) **a** Integration area of the Mn-$L_{2,3}$ edge for calculating the Mn L_3/L_2 ratio. The *red dashed line* shows the Hartree–Slater step function. **b** Mn L_3/L_2 ratio of $SrMnO_{3-\delta}$ thin film with Sr/Mn = 50/50 and 53/47. As shown with *red dashed line*, the Mn L_3/L_2 ratio decreases with increase of the Mn nominal oxidation state

the Sr-excess for SMO (Sr/Mn = 53/47) film can not be accounted for solely by extra SrO planes, i.e., the SMO crystal between the extra SrO planes will have an Sr-excess composition. It is therefore considered that Mn vacancies exist in the SMO crystals, and the presence of Mn vacancies would lead to an increase in the Mn oxidation state. In the case of ionic crystals such as SMO, when vacancies are incorporated, the lattice at the area commonly expands due to electrostatic repulsion [23]. This explains out-of-plane lattice expansion and Mn valence increase in the SMO (Sr/Mn = 53/47) film. Since it is usually very difficult to directly reveal the presence of Mn vacancies, the effects of oxygen vacancies were checked by annealing the specimens at 400 °C for 24 h in air and by measuring the change of the lattice parameters. As shown in Fig. 8, the out-of-plane lattice parameters of post-annealed Sr-excess SMO films were not coincident with that of post-annealed stoichiometric SMO film. This indicates that many Mn vacancies are present in Sr-excess SMO films, which still results in out-of-plane lattice expansion of post-annealed Sr-excess SMO films.

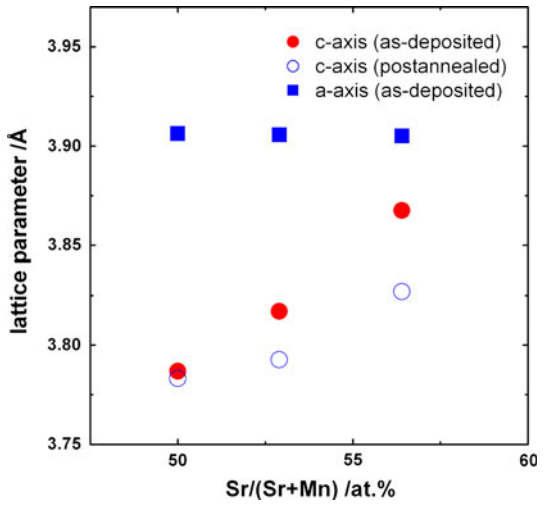

Fig. 8 (Color online) In-plane (*filled squares*) and out-of-plane (*filled circles*) lattice parameters of as-deposited $SrMnO_{3-\delta}$ films with Sr/Mn = 50/50, 53/47, and 56/44. *Opened circles* show the out-of-plane lattice parameters of post-annealed $SrMnO_{3-\delta}$ films. It should be noted here that the out-of-plane lattice parameter for post-annealed stoichiometric SMO film may not be so accurate, because the SMO film was severely cracked during the post annealing

Summary

We revealed the dependency of the cation ratio in SMO films on laser fluence by PLD. The atomic-scale structure and the oxidation state of Mn of the films were carefully investigated. The crystal quality of SMO thin film was found to be closely related to the Sr/Mn ratio. The crystallinity degraded in SMO (Sr/Mn = 45/55) films. On the other hand, epitaxial thin films could be obtained for SMO (Sr/Mn = 50/50, 53/47, and 56/44) films. In Sr-excess SMO film, the expansion of the out-of-plane lattice parameter and an increase in the Mn oxidation state were observed, which is considered to be due to the presence of Mn vacancies.

Acknowledgement A part of this work was supported by the Grant-in-Aid for Scientific Research on Priority Areas "Nano Materials Science for Atomic-scale Modification 474" and Young Scientists (A) 22686059, from the Ministry of Education, Sport, and Technology (MEXT) of Japan, and this study was partially supported by "MACAN Grant No. 233484" project funded by European Framework Programme 7 (FP7).

References

1. Ohnishi T, Lippmaa M, Yamamoto T, Meguro S, Koinuma H (2005) Appl Phys Lett 87:241919
2. Ohnishi T, Shibuya K, Yamamoto T, Lippmaa M (2008) J Appl Phys 103:103703
3. Brooks CM, Kourkoutis LF, Heeg T, Schubert J, Muller DA, Schlom DG (2009) Appl Phys Lett 94:162905

4. Kim YS, Kim DJ, Kim TH, Noh TW, Choi JS, Park BH, Yoon JG (2007) Appl Phys Lett 91:042908
5. Jang HW, Kumar A, Denev S, Biegalski MD, Maksymovych P, Bark CW, Nelson CT, Folkman CM, Baek SH, Balke N, Brooks CM, Tenne DA, Schlom DG, Chen LQ, Pan XQ, Kalinin SV, Gopalan V, Eom CB (2010) Phys Rev Lett 104:197601
6. Tokura Y, Tomioka Y (1999) J Magn Magn Mater 200:1
7. May SJ, Ryan PJ, Robertson JL, Kim JW, Santos TS, Velthuis SGE, Karapetrova E, Zarestky JL, Eckstein JN, Bader SD, Bhattacharya A (2009) Nat Mater 8:892
8. Konishi Y, Fang Z, Izumi M, Manako T, Kasai M, Kuwahara H, Kawasaki M, Terakura K, Tokura Y (1999) J Phys Soc Jpn 68:3790
9. Mitchell JF, Millburn JE, Medarde M, Short S, Jorgensen JD, Fernández-Díaz MT (1998) J Solid State Chem 141:599
10. Gillie LJ, Wright AJ, Hadermann J, Tendeloo GV, Greaves C (2002) J Solid State Chem 167:145
11. Gillie LJ, Wright AJ, Hadermann J, Tendeloo GV, Greaves C (2003) J Solid State Chem 175:188
12. Yang H, Tang YK, Jiang JL, Feng WJ, Wei ZQ, Yao LD, Zhang W, Li QA, Li FY, Jin CQ, Yu RC (2007) J Mater Sci 42:9559. doi:10.1007/s10853-007-1895-0
13. Lee JH, Rabe KM (2010) Phys Rev Lett 104:207204
14. HREM-Filters Lite v1.5.1 (HREM Reseach Inc). Web site: http://www.hremresearch.com
15. Negas T, Roth SJ (1970) J Solid State Chem 1:409
16. Negas T (1973) J Solid State Chem 7:85
17. Kuroda K, Shinozaki K, Uematsu K, Mizutani N, Kato M (1980) J Am Ceram Soc 63(1):109
18. Standard JCPDS diffraction pattern-36-0355 (1995) JCPDS-International Centre for Diffraction Data, PCPDFWIN, v. 1.10
19. Pennycook SJ, Jesson DE (1991) Ultramicroscopy 37:14
20. McCoy M, Grimes R, Lee W (1997) Philos Mag A 75:833
21. Brous J, Fankuchen I, Banks E (1953) Acta Crystallogr 6:67
22. Varela M, Oxley MP, Luo W, Tao J, Watanabe M, Lupini AR, Pantelides ST, Pennycook SJ (2009) Phys Rev B 79:085117
23. Freedman DA, Roundy D, Arias TA (2009) Phys Rev B 80:064108